Experimental Study of Organic Rankine Cycle System and Expander Performance for Heavy-Duty Diesel Engine

Fuhaid Alshammari[a,b*], Apostolos Pesyridis[a],

[a] Brunel University London, Department of Mechanical, Aerospace & Civil Engineering, CAPF – Centre of Advanced Powertrain and Fuels, Uxbridge, UB8 3PH, United Kingdom

[b] University of Hail, Department of Mechanical Engineering, 81481, Hail, Saudi Arabia

Abstract

A small scale organic Rankine cycle system capable of generating electric power using exhaust gas of a 7.25 ℓ heavy duty diesel engine was built and tested. A custom-designed radial inflow turbine was used as an expansion machine, and NOVEC649 was used as the working fluid. In order to maintain steady state operation, a thermal oil loop was installed in the system as an intermediate circuit between the exhaust gas and organic Rankine cycle loop. Compared to the previous study by the authors, the operating conditions were further extended. In addition, the effects of cooling water temperature and working fluid superheating temperature on turbine performance were explored in the current study. The coupled engine-organic Rankine cycle system presented an electrical power, turbine efficiency and thermal efficiency of 9 kW, 35% and 4%, respectively. The results showed that both cooling water temperature and working fluid superheating temperature had a negative impact on the radial turbine performance (generated power and efficiency). The average decrement of the generated power and turbine efficiency were 2.4% and 1.7%, respectively, when increasing the cooling water temperature by 2^oC, and 2.5% and 7.3% when increasing the working fluid superheating temperature by 5^oC. Moreover, the extended tests were beneficiary for validating the proposed performance prediction meanline model developed by the authors in a previous study. The maximum deviation between the measured and predicted turbine efficiency was 3.5%.

Keywords: Waste heat recovery; heavy-duty diesel engine; organic Rankine cycle; experimental testing; cooling water temperature; superheating temperature

*Corresponding author: Fuhaid Alshammari

E-mail: Fu.alshammari@uoh.edu.sa

URL: http://www.uoh.edu.sa/facultymembers/en/FU.ALSHAMMARI/pages/default.aspx

Nomenclature

Variables		**abbreviation**	
h	Enthalpy [kJ/kg]	BK	Blockage factor
m	Mass flow rate [kg/s]	BSFC	Break specific fuel consumption
N	Rotational speed [RPM]	CO2	Carbon dioxide
P	Pressure [kPa]	CTRC	CO2-based transcritical Rankine cycle
T	Temperature [K]	EU	European Union
		EoS	Equation of state
Subscript		FGT	Fixed geometry turbine
0	Stagnation property	GWP	Global warming potential
cr	critical	HDD	Heavy duty diesel engine
is	insentropic	HT-RC	high-temperature loop Rankine cycle
		ICE	Internal combustion engine
Greek Symbols		LT-RC	Low-temperature loop Rankine cycle
η	Efficiency [-]	MFP	Mass flow parameter
		ODP	Ozone depletion potential
		ORC	Organic Ranke cycle

PDE	Positive displacement expander
PR	Pressure ratio
RC	Rankine cycle
WHR	Waste heat recovery

1. Introduction

Carbon dioxide (CO2) emissions of the transportation sector have a significant global impact on air quality and the environment. Therefore, EU legislation sets mandatory emission reduction targets, as the fleet average to be achieved by all heavy duty diesel (HDD) engines was 9% in 2017 compared to 2010 [1]. Among fuel-based applications, transportation burns most of the world's fuel, accounting for more than 67% of the total fuel consumption in the United States [2] and 73% in the United Kingdom in 2013 [3]. Therefore, manufacturers are required to produce more efficient combustions engines. In this regard, waste heat recovery (WHR) technology is one of the promising technologies in recovering the wasted fuel energy

Recently, organic Rankine cycle (ORC) systems as waste heat recovery (WHR) systems in internal combustion engines (ICEs) have received increasing interest. This technology is most widely used in low- to medium-temperature heat sources, typically between 80°C and 350°C, due to the low boiling point of organic fluids compared to steam, which is widely used in large-scale applications. However, further development is still required to implement such technology in modern passenger cars because of the need for compact integration and controllability in the engine [4]. Engine waste heat can be transferred directly through the evaporator to the ORC loop, but in some studies, an intermediate thermal oil loop between the exhaust gases and the ORC is used [5]. Direct heat transfer from the exhaust gases to the organic fluid is often preferred in transport applications as it increases the heat transfer efficiency and reduces the weight of the WHR system, while the thermal oil loop requires an extra heat exchanger and pump. However, cycles with an intermediate oil loop guarantees steady-state conditions for the ORC operation, while any potential decomposition of the working fluid at high exhaust enthalpy conditions can be avoided [5].

Many theoretical studies regarding integrated ORC systems in vehicle powertrain present thermal efficiencies between 6% and 20%. This variation in ORC thermal efficiency mainly depends on the heat sources used in engine operating conditions. In 2012, Katsanos et al. [6] performed a thermodynamic analysis of an ORC system applied on a six-cylinder heavy-duty two stage turbocharged truck diesel engine. The results presented a 20% thermal efficiency of the cycle. The following year, Shu et al. [7] compared three regenerative dual-loop organic Rankine cycle systems are proposed to compare with the simple dual loop organic Rankine cycle, using the wasted heat of the exhaust and engine coolant of a diesel engine. A maximum net output power of 39.67 kW was obtained with the simple dual loop organic Rankine cycle while the other loops presented slightly lower performance due to higher system irreversibilities. Two years later Song and Gu [8] obtained a thermal efficiency equals to 11.8% when recovering the wasted heat in the exhaust gas of an inline six-cylinder turbocharged engine. The following year, the authors [9] investigated the effects of variable geometry turbine performance on the performance on organic Rankine cycle-internal combustion engine (ORC-ICE) system. At the same engine operating point, the cycle with variable geometry turbine presented a 13.9% thermal efficiency compared to 10.5%

when using a fixed geometry turbine. In 2018, several studies were published in the open literature. Yang et al. [10] developed an ORC model to harvest the wasted heat in the exhaust gas of a heavy-duty diesel engine, and presented a thermal efficiency of 6.6%. Rashwan et al. [11] presented a thermodynamic analysis of an organic Rankine cycle integrated with a cascaded closed loop cycle. According to the authors, the cascaded closed loop cycle is considered one of the advanced heat recovery technologies that enhances thermal efficiency significantly. The results showed that thermal efficiency of the cascaded closed loop cycle was 21%, while it was 11% with simple ORC system. Mashadi et al. [12] investigated the feasibility of ORC systems to recover the wasted heat in a 4 cylinder gasoline engine coolant. A thermal efficiency of 18.45% was obtained. More recently, Li et al. [13] investigated the effects of turbine efficiency and working fluid type on the performance of the system. The results showed a maximum thermal efficiency of 12.5% with R236ea as the working fluid. Therefore, as mentioned earlier, thermal efficiencies of ORC systems could not exceed 20% in ICEs. The following paragraph presents a summary of the experimental work of ORC-ICE systems.

Several experimental studies investigating the feasibility of ORC systems as WHR systems in ICEs have been published. In 2007, Honda [14] installed an ORC system on a hybrid vehicle with the vehicle running at constant speed. The results presented a 13.2% improvement in the thermal efficiency compared to the base vehicle. Five years later, Zhang et al. [15] installed a Rankine cycle system on a marine 2-stroke diesel engine and claimed that a 10% efficiency improvement was achieved. In the same year, Hossain and Bari [16] conducted an experiment to measure the available exhaust heat from a 40 kW diesel generator using Rankine cycle. At 40% part load, the additional power developed was 3.4% which resulted in 3.3%

reduction in BSFC. In 2014, Zhang et al. [17] built an experimental system to recover wasted heat in the exhaust gas of a 336 horsepower diesel engine. A single-screw expander and R123 were selected as the expansion machine and working fluid respectively. The results indicated that the maximum power output, ORC efficiency and overall system efficiency were respectively 10.38kW, 6.48% and 43.8%. In the same year, Furukawa et al. [18] conducted an experimental test on the ORC on order to recover the wasted heat in the engine coolant. The fuel consumption decreased by 7.5%. A year later, Galindo et al. [19] tested an ORC system integrated in a 2 liter turbocharged gasoline engine using ethanol as working fluid and swash-plate expander as the expansion machine. A maximum real Rankine efficiency value of 6% was obtained. In 2016, three experimental studies were published. Yu et al. [20] constructed a cascaded system that comprises a steam Rankine cycle (RC) as the high-temperature loop (HT-RC) and an organic Rankine cycle as the low-temperature loop (LT-ORC) for waste heat recovery from an in-line, six cylinders diesel engine. Comparing to the basic diesel engine, the power increment reaches up to 5.6% by equipping the cascaded system. Guillaume et al. [21] used exhaust gases of a truck diesel engine as the heat source for their ORC system. They used a radial inflow turbine as the expansion machine and two working fluids: R245fa and R1233zd. However, the employed turbine was developed mainly using components modified from truck turbocharger designs. Also, the heat wasted by the truck through the exhaust gases is simulated using an electric oil boiler coupled to the ORC loop. The maximum electric power and turbine efficiency were 2.8 kW (using R245fa) and 32% (using R1233zd), respectively. AVL, FPT and Iveco [22] built an ORC system to harvest the wasted heat in the exhaust gas of a 4-stroke diesel engine. The tests were run on public roads and the results showed that the fuel consumption could be reduced by 2.5–3.4%. The following year, two experimental studies on ORC-ICE systems were published. Sellers [23] evaluated the benefits of ORC systems in recovering the wasted heat in the jacket water of a 12 cylinder ship engine. The results showed that the largest kilowatt hour value of 78,001 was produced during the first voyage from Asia to the USA east coast. Shi et al. [24] constructed four CO2-based transcritical Rankine cycle (CTRC) systems (basic ORC, ORC with regenerator, ORC with coolant preheater and ORC with both the preheater and the regenerator) with kW-scale power output to recover waste heat from both exhaust gas and coolant water of an in-line, six cylinders diesel engine. However, the authors applied expansion valve instead of turbine. Among the four configurations, the ORC with both the preheater and the regenerator showed the highest net power output and thermal efficiency, whose estimation reach up to 3.47 kW and 7.8%, respectively. In 2018, the authors [25] have built an ORC system to recover the wasted heat in a a 7.25ℓ Yuchai engine at highly off-design conditions. An intermediate thermal oil loop has been placed between the heavy duty diesel engine the ORC system in order to ensure steady operation while keeping the fluid temperature below the decomposition one. The maximum obtained thermal efficiency has been 4%, and an electrical power of 6 kW has been generated. More recently, Linnemann et al. [26] tested an ORC system, toluene as a working fluid, driven by biogas waste heat with focusing on the design and testing of multi-coil helical evaporator performance. According to the authors, the turbine was not operational thus, the working fluid was carried through a bypass and expanded with an orifice plate, before entering the recuperator. that the predicted values of the overall heat transfer coefficient and the shell side Nusselt number are in good agreement with experimental data, showing a maximum deviation of 5.5%. The brief literature survey indicates that ORC system is a promising WHR technology An extensive review of automotive ORC systems can be found in a previous work by the authors [27].

Radial turbine is a component within a larger system (i.e., ORC). Therefore, cycle analysis should be considered during the turbine design stage. Moreover, in heat sources such as ICEs, the thermodynamic parameters of the exhaust gas, such as mass flow rate and temperature, can vary widely with time. This variance causes heat sources to become unstable and uncontrollable. Therefore, the performance behaviour of a turbine when the machine runs at off-design rotational speeds, mass flow rates, and pressure ratios should be accurately predicted. However, there is a scarcity of information in open literature regarding the mean-line modelling to obtain the off-design performance of ORC turbines, a point confirmed in White [28] and Wong [29]. Several air turbine models were developed in literature such as [30-35]. However, no consideration of real fluid properties were taken into account in the aforementioned studies, rather, ideal gas correlations were applied. The thermodynamic properties of high-density fluids, such as organic fluids, are different from those of ideal gases. For instance, organic fluids have high molecular weight, low boiling points and low speed of sound. In addition, ORC radial turbines present high expansion ratio and Mach number at the stator exit due to the frequently changing specific volume, which results in supersonic flows. This outcome necessitates the use of a real EoS rather than the traditionally adopted Mach relationships for ideal gas. The thermodynamic properties at each station must likewise be checked simultaneously through the turbine stage. For this investigation, a novel performance prediction method for ORC radial-inflow turbine was developed by the authors in a previous work [36].

The brief literature review in the 3rd and 4th paragraphs, and the literature review study by the authors [27] show that only Guillaume et al. [21] and the previous study of the authors [25] examined the feasibility of ORC systems in automotive applications with radial turbines as expansion machines. Even though, the turbine in Guillaume et al. [21] was developed using components of truck turbochargers. Also, they applied an electric oil boiler as the heat source rather than real engine exhaust gas. The coupling of ORC systems with real heavy duty diesel engine an area in which little available literature exists. Moreover, according to the literature review study [27] and the brief literature review in the 3rd and 4th paragraphs, effects of cooling water temperature and working fluid superheating temperature on turbine performance have not yet been discussed, neither theoretically nor experimentally. Therefore, further testing is performed in the current study in order to study the effects of cooling water temperature on the radial turbine performance. In addition, one of the objectives of the current study is to accurately validate the proposed meanline model in Alshammari et al.[36]. The latter is very essential since ORC radial turbines experience choking conditions due to high pressure ratio and low speed of sound of organic fluids. Besides validating the meanline model, the present study highlights the effects of input parameters on the turbine off-design performance and mass flow rate.

2. Test Rig

An experimental facility of an Organic Rankine Cycle coupled to an Internal Combustion Engine is tested in order to investigate the feasibility of ORC as WHR system in ICEs. The results of tests are also used to validate the novel meanline model presented by the authors in [36]. The WHR system is presented in Fig. 1. A photograph of the ORC skid with main components identified is presented in Fig. 2.

The test rig consists of the heavy duty diesel engine, thermal oil loop, ORC loop and cooling loop. The diesel engine and ORC loop are briefly presented in this study, as they are detailed in Alshammari et al. [25].

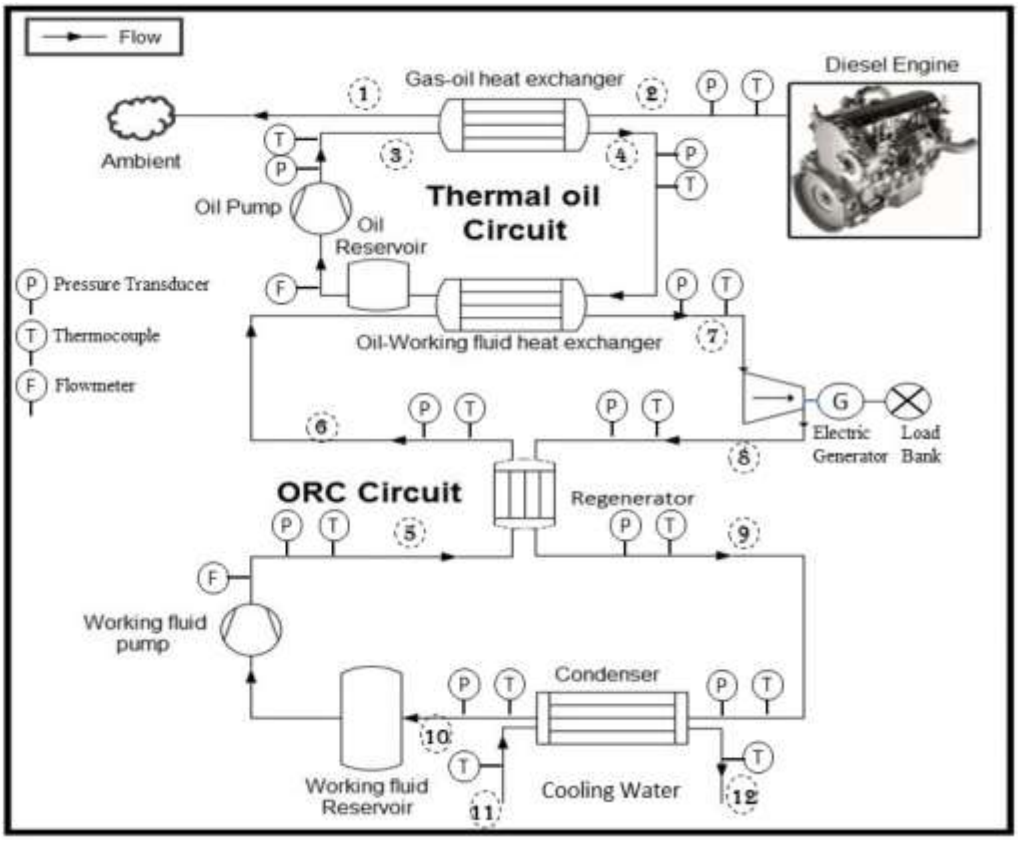

Fig. 1: Experimental ORC installation diagram

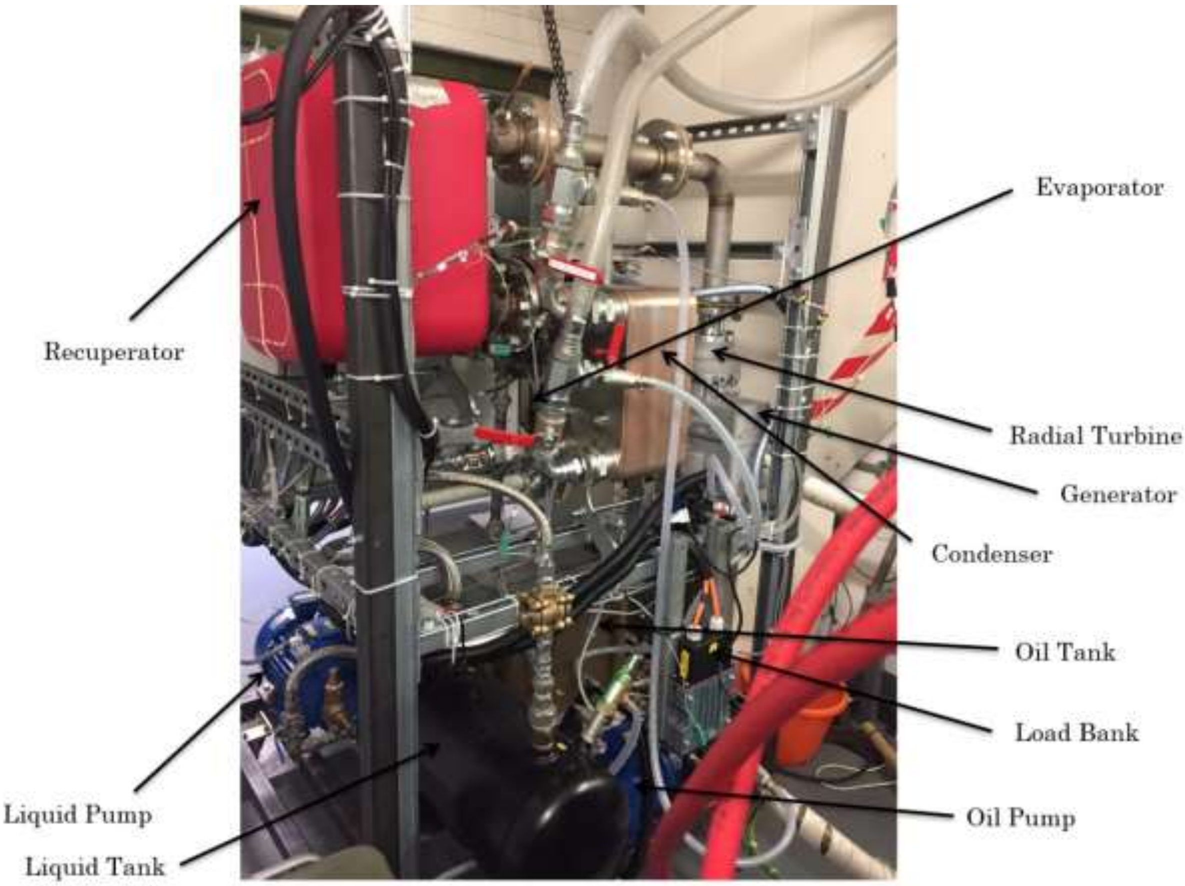

Fig. 2: Photograph of experimental ORC installation

2.1 Fluid Selection

The choice of working fluid for an ORC system is of great importance for the cycle efficiency and net work. ORC systems should only utilise working fluids with low global warming potential (GWP) and ozone depletion potential (ODP) [39]. Compared to steam (in conventional Rankine cycle), organic fluids exhibit unique advantages because they are better adapted to low heat source temperatures, enabling ORC systems to efficiently produce shaft work from low to medium temperature heat sources of up to 370 °C [40]. Compared to conventional Rankine cycles, a smaller plant size will be produced when organic fluids are used because of their high density. The higher the density is, the lower the volumetric flow rate is and, subsequently, the smaller the component size becomes. The selection of working fluid is determined by the application and the waste heat level [37]. Based on the slope of the saturation vapour line, as shown in Fig. 3, working fluids can be classified into three groups: wet, dry and isentropic. Dry and isentropic fluids have enormous advantages for turbo-machinery expanders because they leave the expander as superheated vapour and eliminate the corrosion that results from liquid droplets that impinge on the turbine blades during the expansion [38]. Another advantage is that overheating the vapour before entering the expander is not required, which means a small and cheap heat exchanger can be used. Moreover, a superheated apparatus is not required when using dry and isentropic fluids [39]. However, if the fluid is too dry, the expanded vapour will leave the turbine with substantial superheat, which is a waste and adds to the cooling load in the condenser.

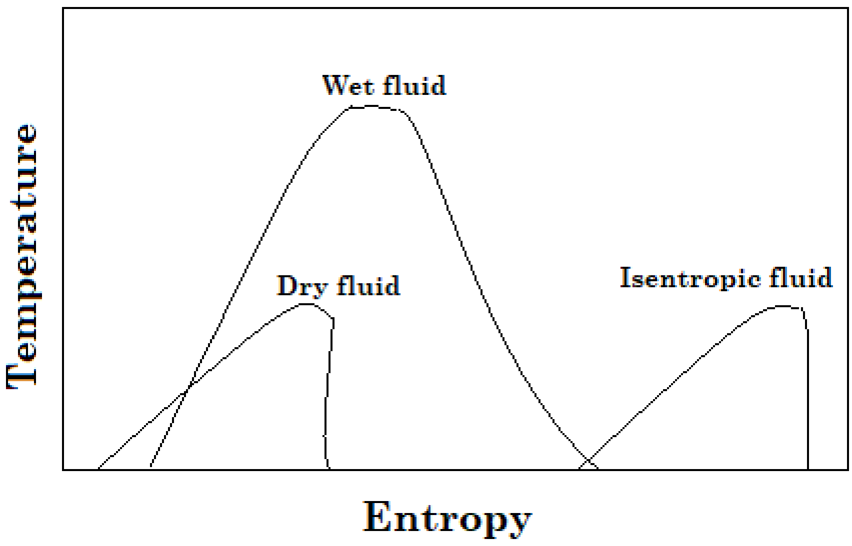

Fig. 3: Types of working fluids

In order to come up with the optimum fluid for the current application, the authors [40] proposed novel method for selecting the proper working fluid for the current application considering thermodynamic properties, radial turbine speed and evaporator heat transfer surface. Using the aforementioned method, the authors further investigated the potential of NOVEC 649 as a working fluid for the current application [41]. The results showed that NOVEC649 produced lower back pressure at the evaporator exit and lower turbine rotational speed, which positively affects the electric generator cost. In addition, NOVEC649 is an effective heat transfer fluid that can be utilized in applications such as ORC where non-flammability or environmental factors are a consideration [42]. The thermos-physical properties of NOVEC649 are presented in Table 1.

Table 1: Properties of NOVEC649

Fluid	Chemical Formula	Molecular Weight (g/mol)	T_{cr} (K)	P_{cr} (bar)	Boiling Point (K)	Molar Mass (g/kmol)	GWP	ODP
Novec649	$CF_3CF_2C(O)CF(CF_3)_2$	316	441.81	18.69	322.2	316.04	1	0

2.2 The heavy duty engine (Heat source)

A photograph of the heavy duty diesel engine applied in the current study is shown in Fig. 4. The diesel engine used in tests is a 7.25ℓ turbocharged, direct injection Yuchai engine with a 17.5:1 compression ratio. The maximum engine torque is 1100 Nm at 1400-1600 rpm and 100% load. The maximum engine power is 206 kW at 2300 rpm and 100% load. However, the engine was not able to run at full load because of the technical issues of the dynamometer. The maximum obtained power output during the tests was nearly 40% of the maximum engine power. This technical issue can be considered as a positive point and more practical since the ORC system rarely operates at the design conditions in automotive applications. In this study, the engine exhaust gas is used as the heat source since it contains the largest portion of wasted heat, which is approximately 20%–42% of the total wasted heat [43], and high exergetic content [44].

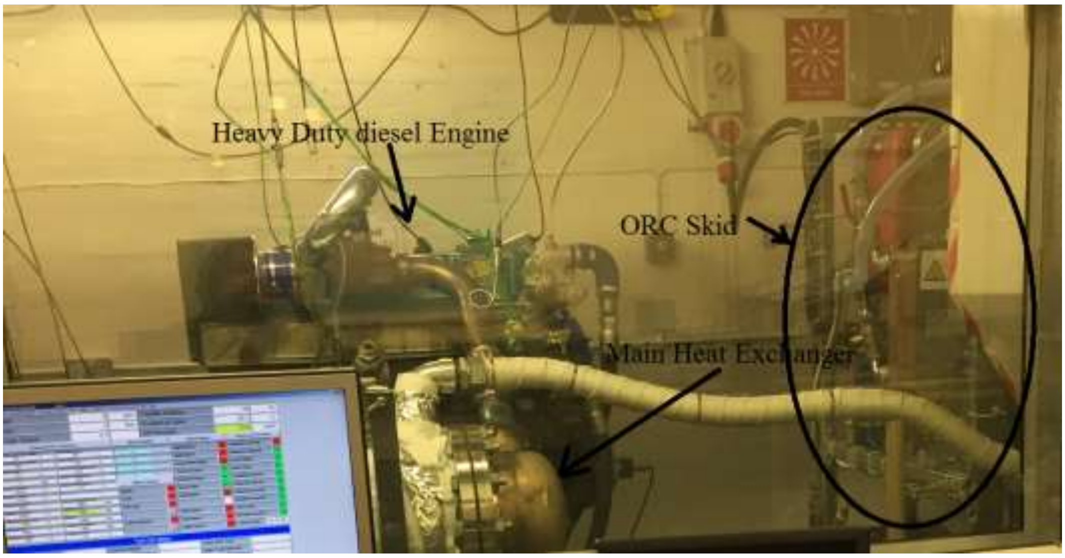

Fig. 4: Photograph of the 7.2 l heavy duty diesel engine (heat source)

2.3 Thermal oil loop

The intermediate thermal oil loop is placed between the exhaust gas of the engine and the ORC system via the main heat exchanger as shown in Fig. 4. The thermal oil loop requires two more components i.e. heat exchanger and pump which results in heavier system. However, the thermal oil loop assures steady-state conditions for the ORC operation, and is beneficial in order to avoid any potential decomposition of the working fluid at high exhaust enthalpy operations. In addition, the combination of ORC-thermal oil assures stabilizing the thermal oil temperature in the evaporator. The thermal oil is a synthetic organic heat transfer fluid contains a mixture of diphenylethane and alkylated aromatics. It exhibits better thermal stability, particularly at the upper end of hot oil's use range, and significantly better low-temperature pumpability. It's critical temperature and pressure are 489^oC and 24 bar, respectively.

2.4 Organic Rankine cyle loop

Fig. 2 presents a photograph for the experimental set up of the ORC system used in this study. In the main heat exchanger (Fig. 4), heat transfers from the exhaust gas of the diesel engine to thermal oil. Then, the hot thermal oil passes through the evaporator to exchange heat with working fluid. After that, the vapour working fluid flows into the radial turbine where the enthalpy is converted to effective work. Then, the fluid enters the recuperator to use the still heat in the working fluid. In order for the fluid to be transformed back to the liquid phase, it flows into the condenser where the cooling circuit starts. The liquid NOVEC649 is then pumped to the evaporator and the cycle starts again. Fig. 5 shows the radial turbine parts i.e. volute, stator and rotor. Fig. 6 presents the coupled turbo-generator unit. More information about the specifications of the ORC components and the instrumentations can be found in Alshammari et al. [25].

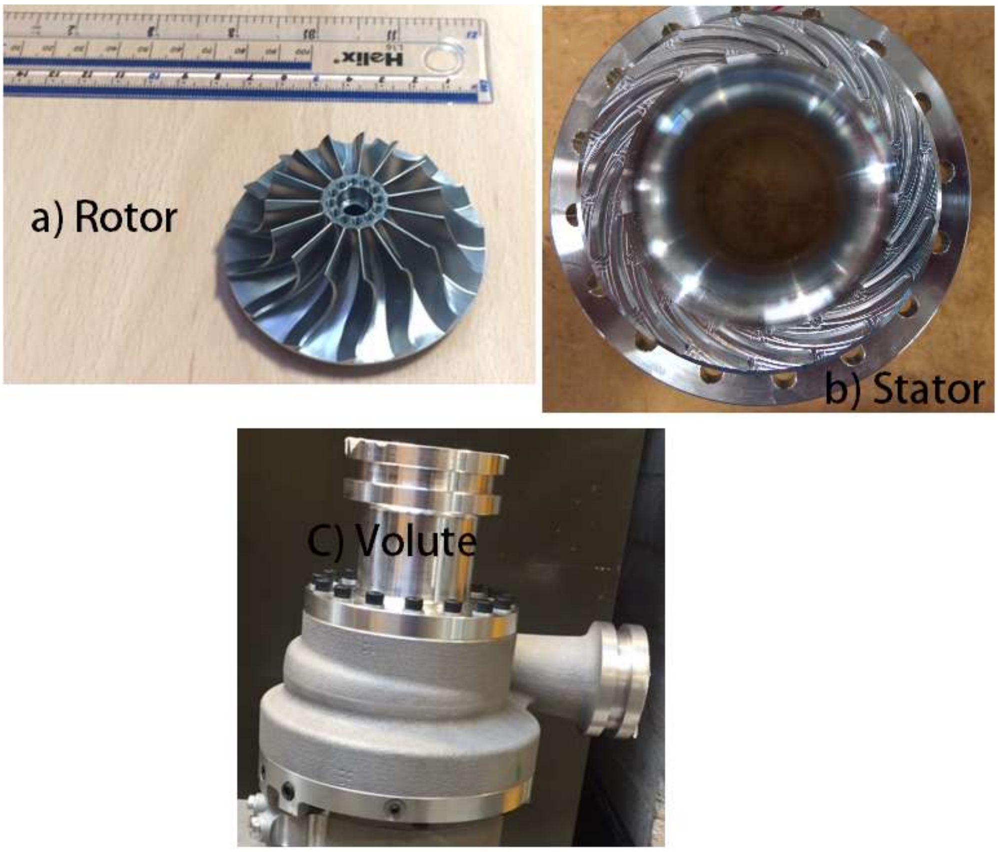

Fig. 5: Manufactured radial inflow turbine

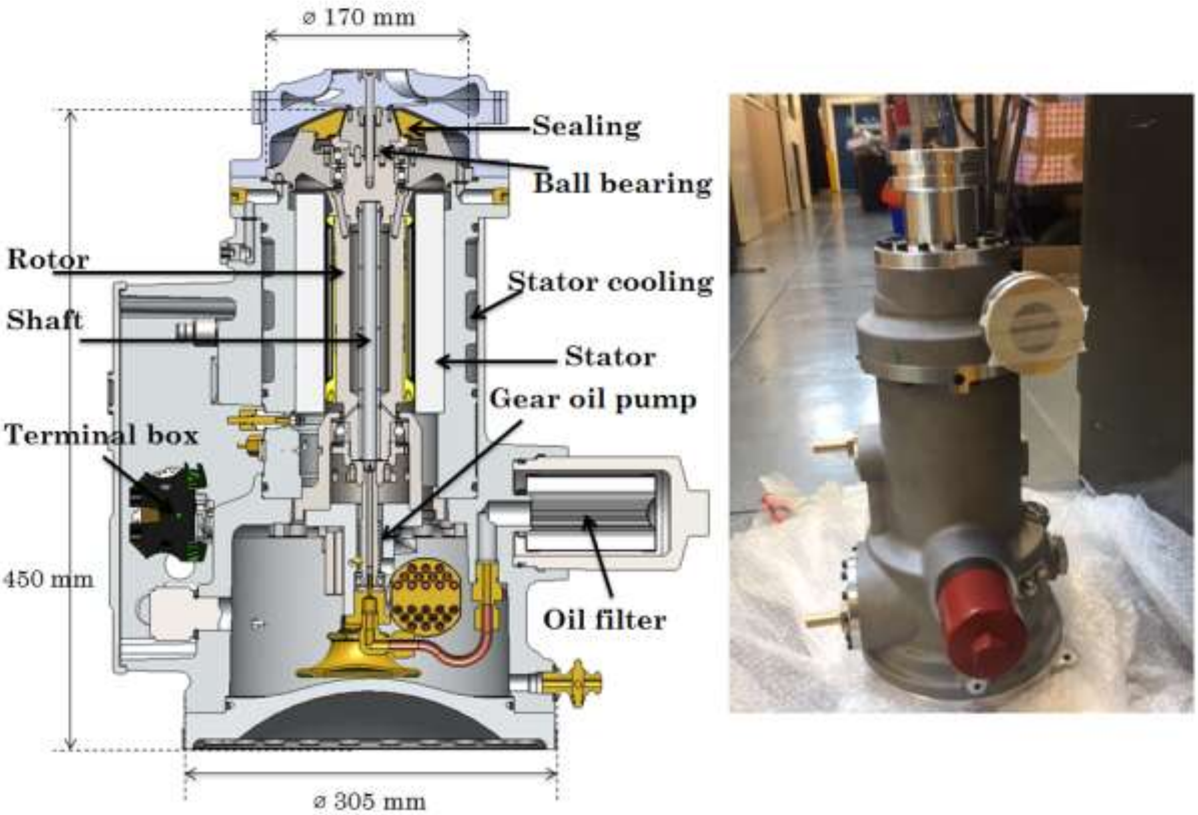

Fig. 6: Electrical generator (coupled to turbine)

2.5 Cooling loop

The cooling loop is a water circuit linked to the condenser in order to remove the heat from condenser to environment, where the state of fluid changes from vapour to liquid. The cooling water inlet temperature changes based on the outside temperature. The tests were run from mid of June to end of July at Brunel University London. The average ambient temperature ranges from $18^{o}C$ to $26^{o}C$. The condenser unit is a counter current flow, brazed plate heat exchanger. The counter current configuration in the condenser is beneficial to ensure that saturated liquid leaves the condenser, thereby, allowing the working fluid pump to operate more efficiently.

3. Mean-line Modelling

Although the ORC system is a promising WHR technology, its cycle efficiency is low due to the low working temperatures. Therefore, designing an efficient turbine and predicting its performance are of great importance to avoid further efficiency reductions. In addition, the thermodynamic properties of heat sources are variable, thus making the prediction of turbine performance at different operating conditions even more important at the design phase.

Supersonic flow is likely to take place in ORC turbines operating due to the high operating pressure ratio and low speed of sound of the organic fluid. Therefore, the corrected mass flow parameter (MFP) is applied instead of the real mass flow rate. In this case, the mass flow rate relies only on the corrected mass flow rate and the operating conditions regardless of the turbine speed and enthalpy drop, as shown in equation (1). This is because, for Mach numbers greater than unity, the mass flow rate remains constant for any pressure ratio equal or greater than the choked value. So, when choking takes place at the blade raw, the choked mass flow is kept fixed. Then, the velocity triangle is solved using the choking mass flowrate value without the described iteration process presented in Fig. 7.

$$MFP = \frac{MFR\sqrt{T_{01}}}{P_{01}} \tag{1}$$

The performance of the turbine is measured using bulk properties for the total-to-total isentropic efficiency definition as shown in equation (2), where "in" and "ex" indicates turbine inlet and exit, respectively. The detailed mathematical model can be found in Alshammari et al. [36].

$$Turbine\ Efficiency = \frac{h_{01} - h_{05}}{h_{01} - h_{05,\mathrm{is}}} \tag{2}$$

Table 2 presents input parameters and performance of the custom-designed radial inflow turbine at the design point.

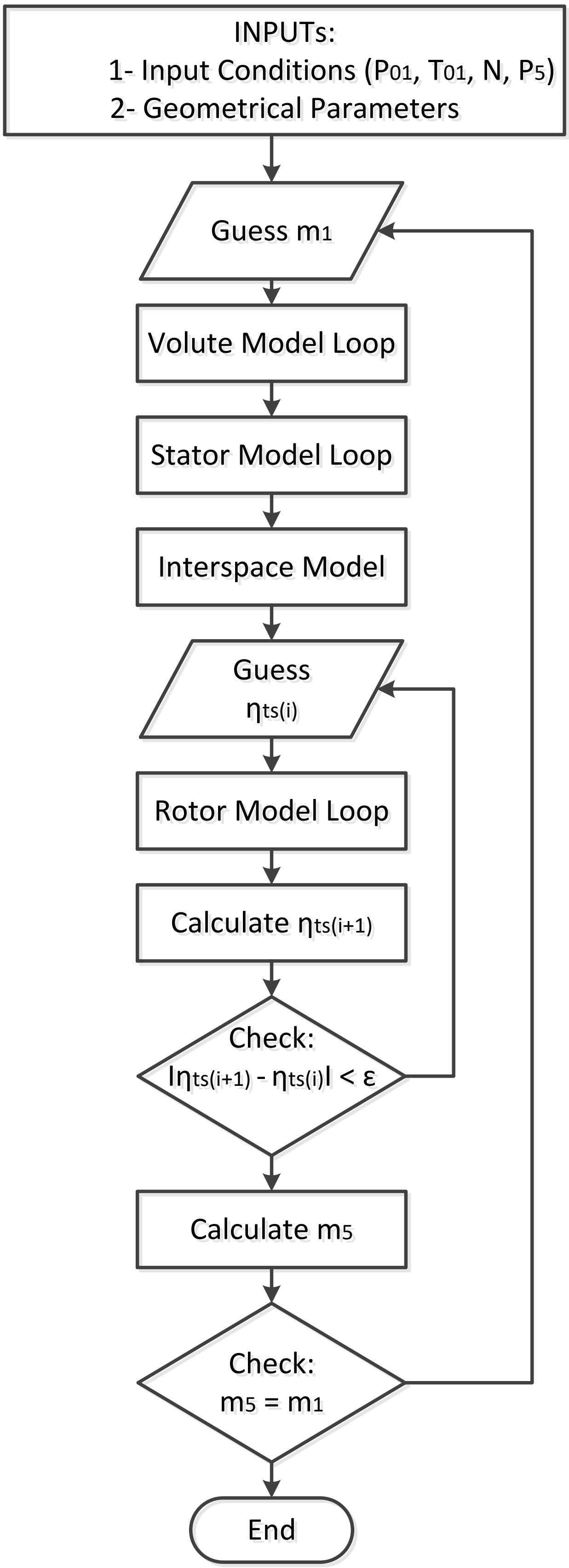

Fig. 7: Flowchart of the performance prediction meanline model [36]

Table 2: Turbine parameters at design point

parameter	Value	Unit
Turbine inlet total pressure	9	bar
Turbine inlet total temperature	471.5	K
Turbine exit static pressure	1.30	bar
Turbine speed	40,000	rpm
Working fluid mass flow rate	0.8	Kg/s
Turbine efficiency	74.4	%
Turbine power output	13.6	kW

4. Results and Discussion

The first part of this section covers the results of the ORC testing, and the second part covers the validation of the performance prediction meanline model.

4.1 Experimental results of the organic Rankine cycle system

It is worth mentioning that the recording of the test data was initiated once thermal equilibrium was achieved. Therefore, the time (x-axis) shown in the figures in this section is the time after recording and not the time from the start of the test.

4.1.1 Steady state operation

Fig. 8 assures the steady-state operation of the system through entire period of testing. The figure presents the temperature at the turbine inlet, evaporation pressure, and condensation pressure. The maximum variation of the temperature is 0.65% for about 37 minutes of testing which is negligible. The pressure, on the other hand, is oscillating but with very small variation. The maximum variations of evaporation and condensation pressures are 2.5% and 1.6%, respectively.

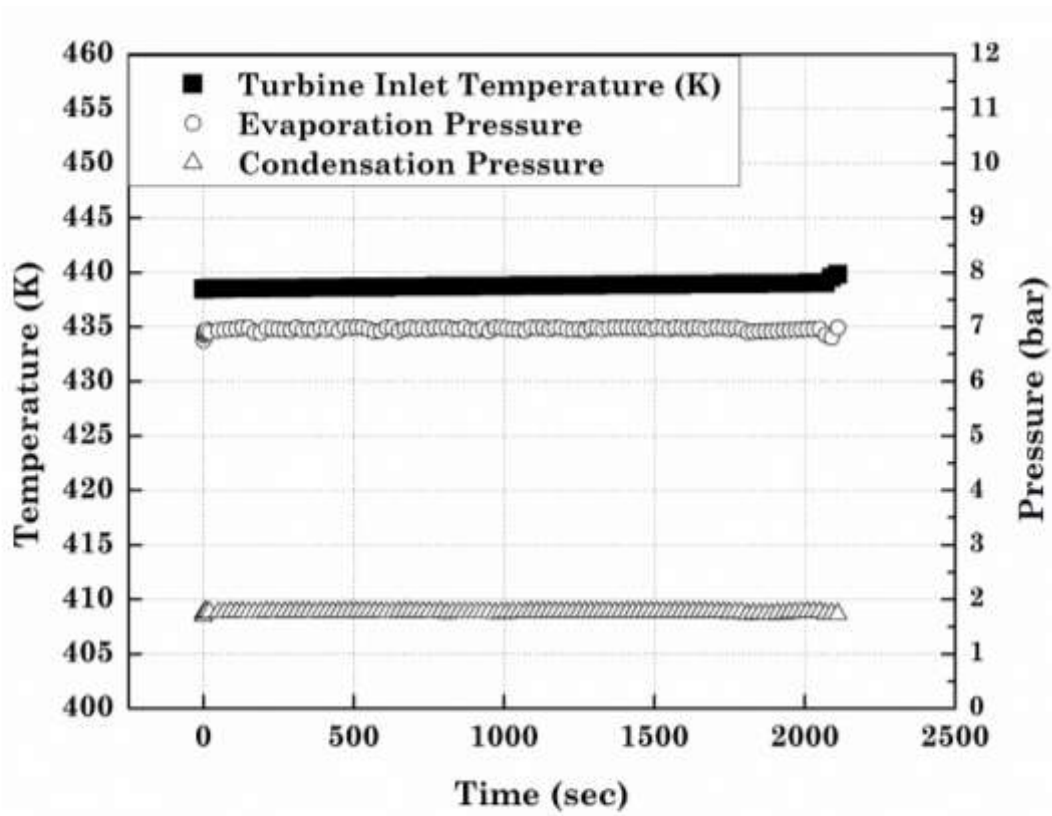

Fig. 8: Steady state conditions during testing

4.1.2 Generated power and pump power

Fig. 9 shows the variations of pump power and generated power by the generator with mass flow rates. The working fluid pump is connected with an inverter to adjust the pump rotational speed by converting the frequency, which controls the flow rate of the working fluid through the cycle. Obviously, the figure shows an increasing trend for both pump power consumption and generated power with increasing mass flow rate of the NOVEC649. The pump power increases from 177 W to 343.5 W as the mass flow rate of the working fluid increases from 0.057 kg/s to 0.75 kg/s. The generated power increased from 200 W to 9100 kW. Further increase in mass flow rate (beyond 0.75 kg/s), results in a gradual decrease in the generated power due to the increased pump power while the generated power remains constant.

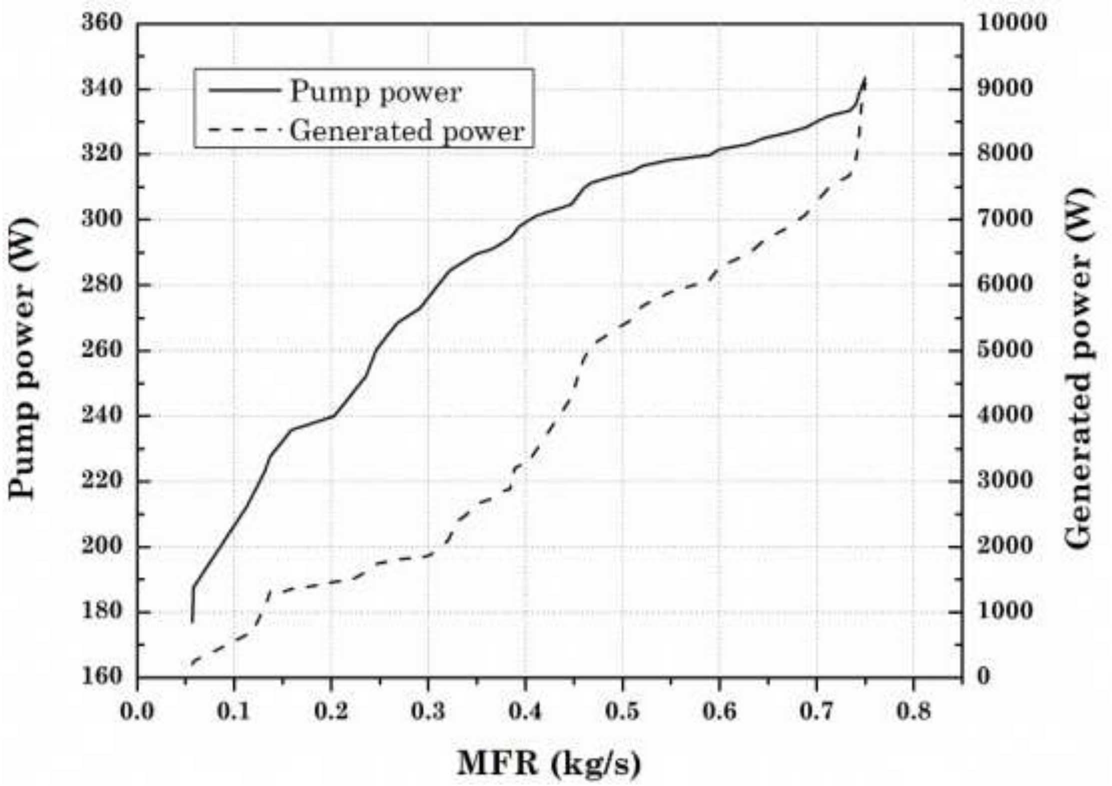

Fig. 9: Generator power and pump power with mass flow rate

4.1.3 Cycle and turbine efficiencies

The cycle and turbine efficiencies with time are depicted in Fig. 10. The average cycle thermal efficiency is 4% ($\pm 0.5\%$), while the turbine efficiency presents larger variations with an average value of 34% ($\pm 1.38\%$). The cycle and turbine efficiencies are recorded with pressure ratio equals to 4.85. The recorded efficiencies are way below the designed values (Table 2). However, this is expected since the system runs at substantially off-design conditions (due to the technical issue of the engine dynamometer as mentioned in section 2.2), at which the peak efficiency of the radial turbine was 34% at 20,000 rpm (instead of 74.4% at 40,000 rpm at the design point). Therefore, the maximum thermal efficiency of the cycle was 4.3% instead of 9.3% at the design point.

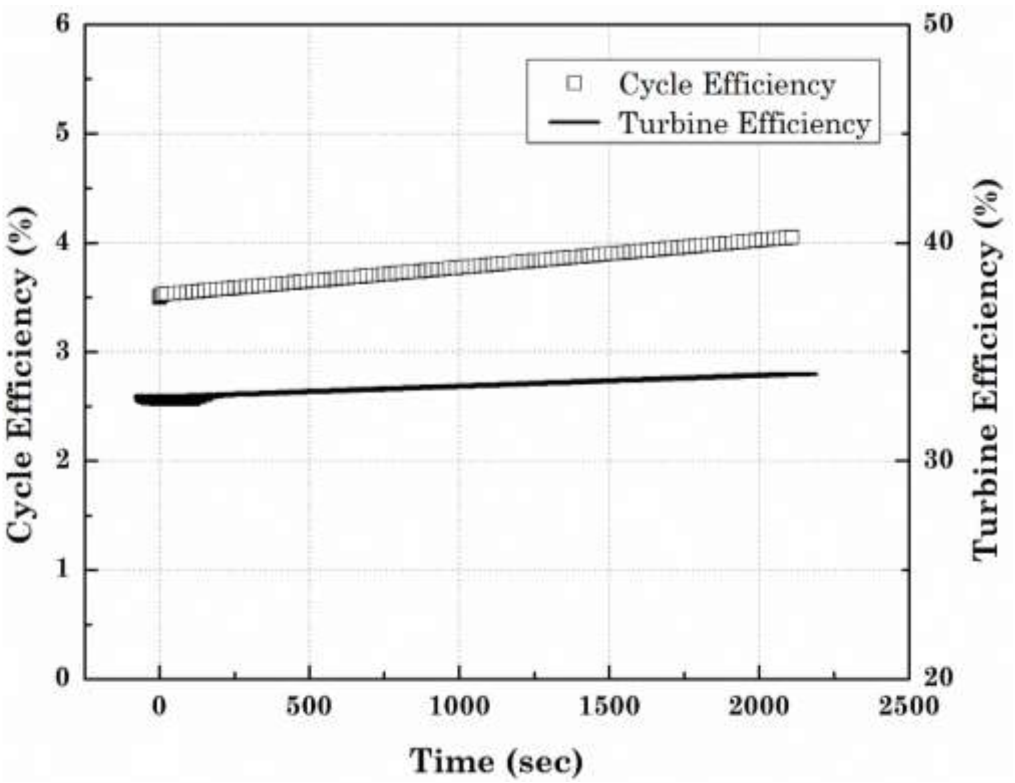

Fig. 10: cycle and turbine efficiencies during entire period of testing

4.1.4 Effects of cooling water temperature

The cooling water temperature depends on the outside temperature since the cooling tower is roof-mounted. Therefore, the tests were run at various times of the day from mid of June to end of July, where the temperature ranged from

18^oC to 26^o. To ensure accurate results, the heavy-duty diesel engine, and hence the thermal oil, was run at constant conditions i.e. constant temperature and mass flow rate for all tests. In addition, the cooling water flow rate was kept constant. The results are presented in Fig. 11 and Fig. 12.

Fig. 11 obviously shows that both generated power and turbine efficiency decreases with increasing the cooling water temperature. The generated power decreases due to the decreasing pressure ratio as shown in Fig. 12. The turbine pressure ratio decreases since the condensing pressure increases (as the cooling water temperature increases) which increases the turbine exit pressure. Although the evaporation pressure also increases, the increase rate is lower than the condensation pressure. The turbine efficiency decreases due to the increased pressure at the turbine exit. Fig. 11 shows that increasing cooling water temperature by 2^o C resulted in average decrement of 2.4% in the generated electrical power and 1.7% in the turbine efficiency.

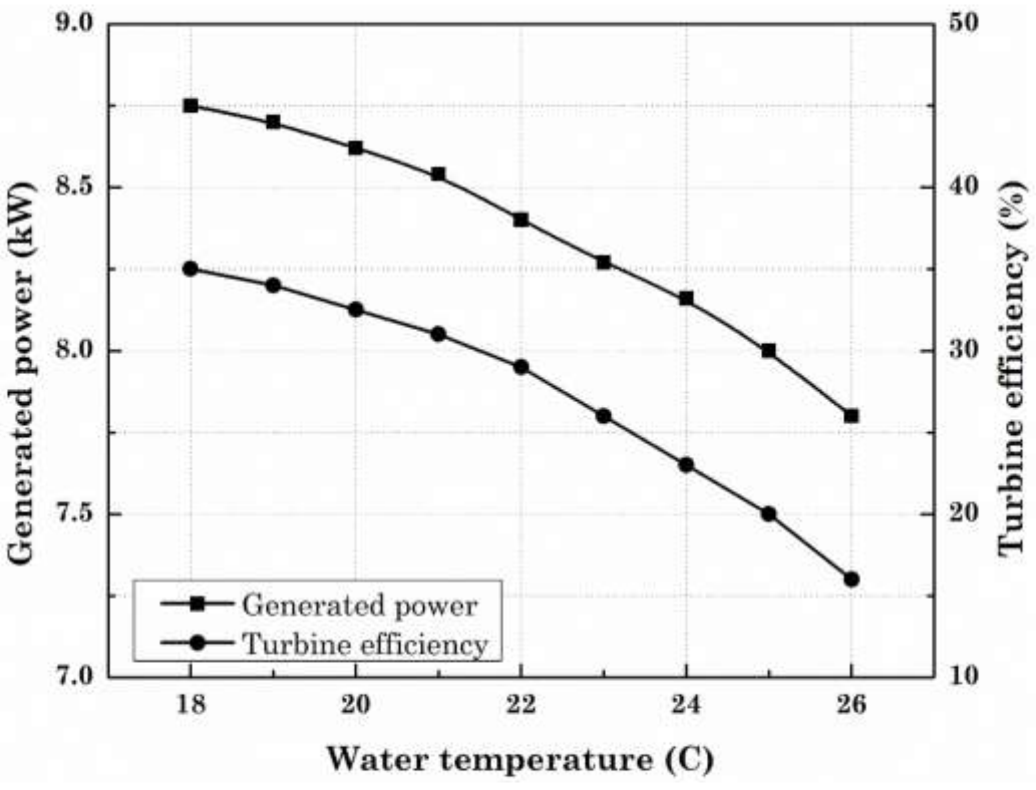

Fig. 11: Generated power by generator and turbine efficiency with increasing cooling water temperature (heat sink).

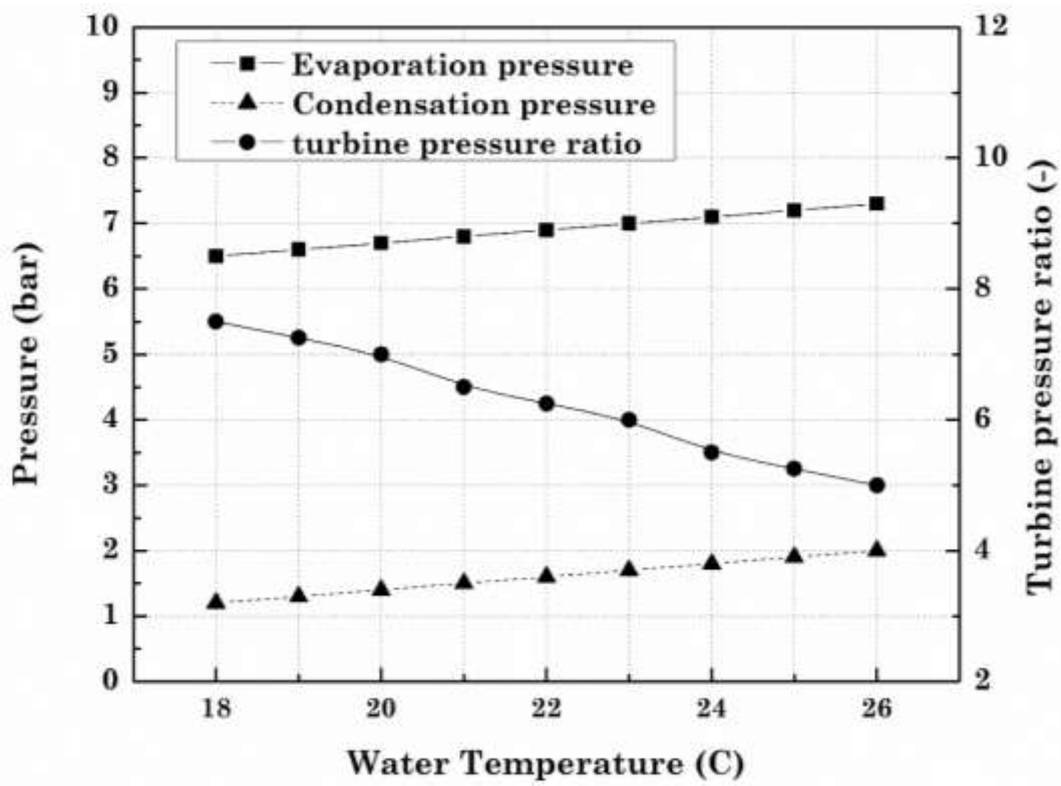

Fig. 12: Evaporation pressure, condensation pressure and turbine pressure ratio with increasing cooling water temperature (heat sink).

4.1.5 Effects of superheating temperature

The working fluid used in the testing (NOVEC649) is a dry fluid. Therefore, more attention should be paid to the superheating temperature. In case of excessive superheating, the expanded vapour would leave the turbine with a substantial superheat, which is a waste and adds to the cooling load in the condenser. The effects of the superheating temperature on the system is shown in Fig. 13 and Fig. 14. To ensure accurate results, the working fluid mass flow rate, and cooling water flow capacity and temperature were kept constant during all tests.

In order to increase the superheating temperature, the evaporation pressure should be increased. This can be obtained by decreasing the speed of working fluid pump. Decreasing the evaporation pressure results in decreasing turbine pressure ratio since superheating temperature increases as shown in Fig. 14. As a result of the decreasing pressure ratio, the generated power and turbine efficiency also decrease as shown in Fig. 13. It is worth mentioning that the condensation pressure is nearly constant due to the constant temperature and flow capacity of cooling water. Fig. 13 shows that increasing NOVEC 649 superheating temperature by $5^{o}C$ resulted in an average decrementt of 2.5% in the generated electrical power and 7.3% in the turbine efficiency.

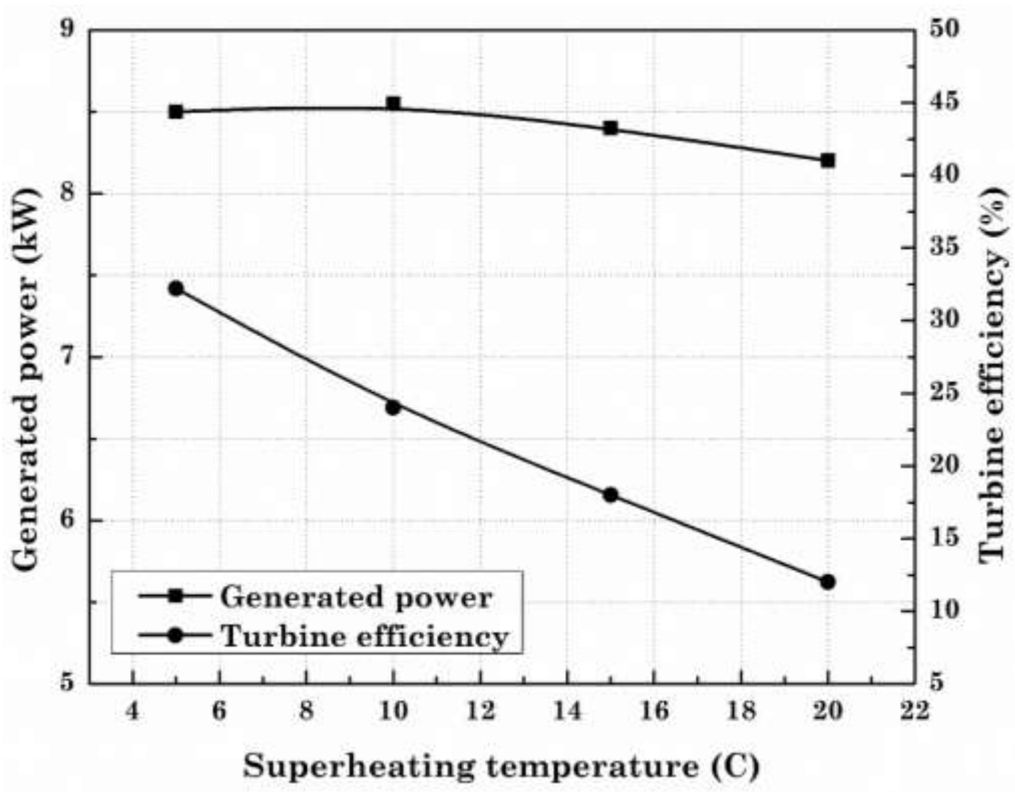

Fig. 13: Generated power by generator and turbine efficiency with increasing superheating temperature

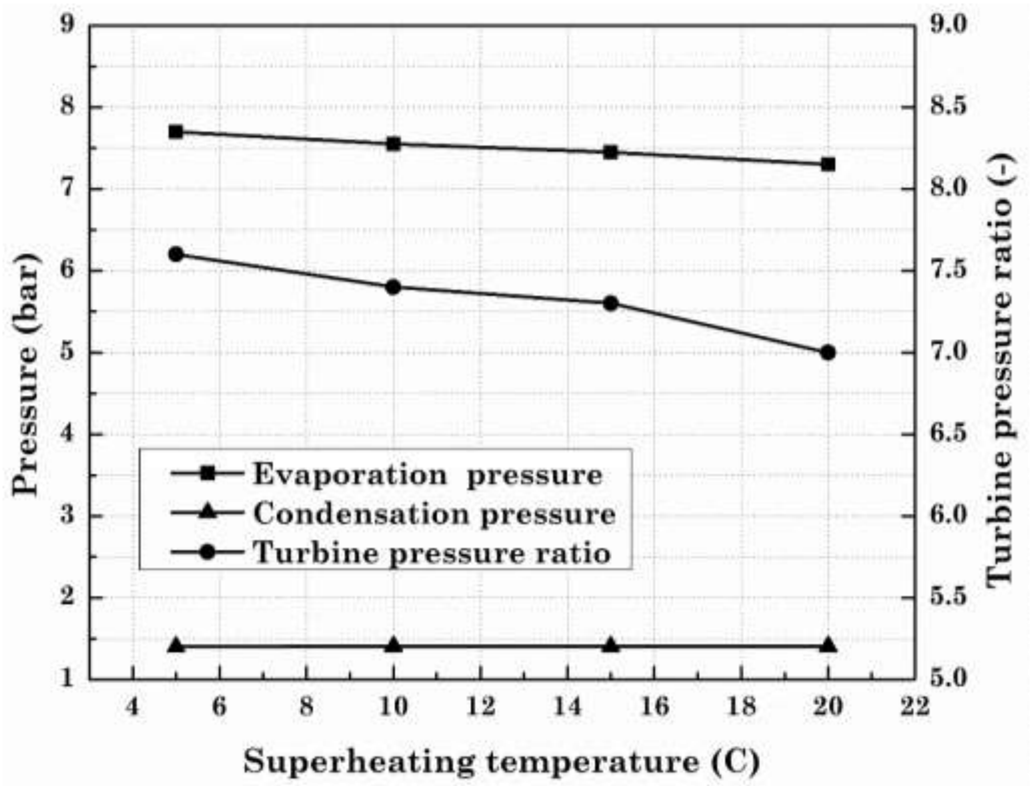

Fig. 14: Evaporation pressure, condensation pressure and turbine pressure ratio with increasing superheating temperature

4.2 Parametric study of the meanline model

It is of great importance to carry out a parametric study of the meanline model prior to validation in order to evaluate the effects of the empirical input parameters that are controlled by the user. These input parameters are stator and rotor blockage factors, stator and rotor deviation angles, and rotor incidence angle.

Fig. 15 presents the effect of the blockage factors of the stator and rotor on the turbine mass flow rate and efficiency. Clearly, increasing the stator blockage has critical impact on the MFR since the flow area decreases by increasing the stator blockage factor. Increasing the blockage factor from 0 to 0.2 results in 20% reduction in the mass flow rate (MFR). On the other hand, turbine efficiency is insignificantly affected by increasing the stator blockage factor with a maximum reduction of 0.46% when the blockage factor increases from 0 to 0.2. This slight effect is related to the change in the incidence angle which results in higher absolute velocity of the flow at the stator exit.

Rotor blockage factor has much less but non-negligible effect on the mass flow rate. Larger blockage factors results in narrower flow path, and hence, lower flow capacities. The efficiency, on the other hand, is relatively sensitive to the rotor blockage due to, beside the reduction in MFR, the increased kinetic energy loss at the rotor exit. As the blockage increases from 0 to 0.2, the MFR and efficiency decrease by 1.3% and 6.27%, respectively.

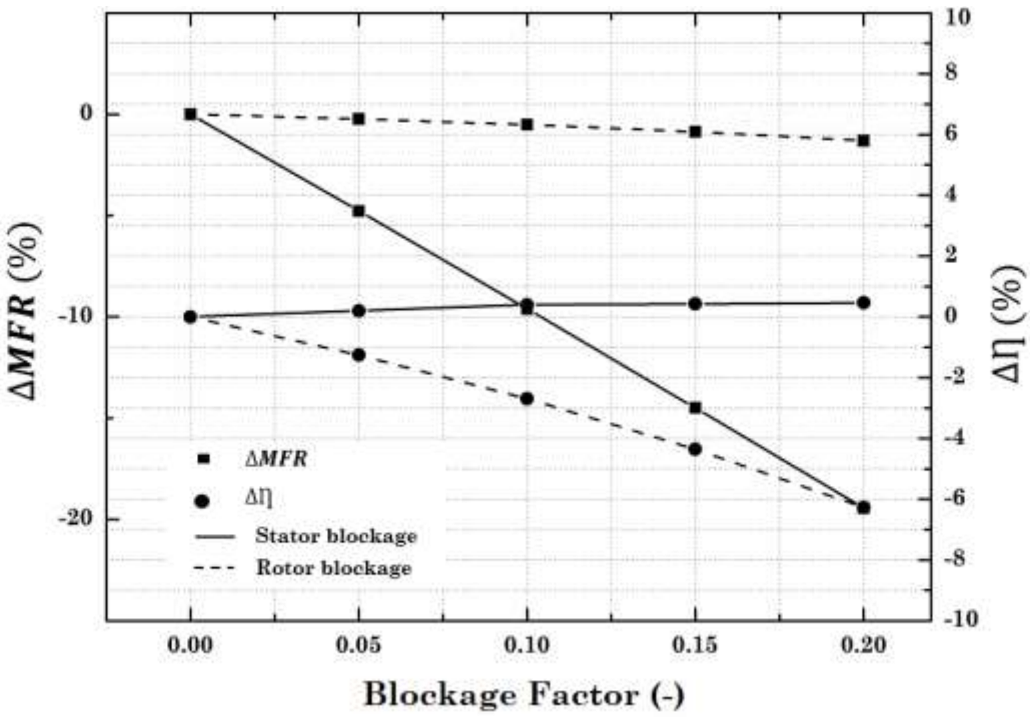

Fig. 15: Deviation of mass flow rate and turbine efficiency versus blockage factors

Fig. 16 presents the effect of the deviation angles on the turbine flow capacity and efficiency. The figure obviously shows that the turbine mass flow rate is very sensitive to the stator deviation angle. As the angle increases from 0 to 2, the mass flow rate decreases by 12%. Changing the deviation angle in the negative direction, from 0 to -2, the mass flow rate increases by 12%. The relationship between the mass flow rate and the stator deviation angle is related to the definition of the mass flow rate at the stator exit. The deviation angle is defined as the difference between the vane angle (setting angle) and the flow angle. As the flow angle moves towards the negative direction (the deviation moves towards the positive direction), the mass flow rate significantly decreases, and vice versa. Fig. 16 also indicates that the stator deviation angle has moderate impact on the turbine efficiency. As the deviation angles moves to the negative direction, the Mach number increases at stator exit, as stated by Benson [45] and Pullen et al.[46], which results in lower turbine efficiency.

The turbine flow rate and efficiency are also investigated by changing the rotor deviation angle by $\pm 2^{o}$. It is obvious that the rotor deviation angle has no impact on the mass flow rate while its impact on the turbine efficiency is small but not negligible. The efficiency decreases with positive rotor deviation angles and increases with positive rotor deviation angles. This is explained by the increase and decrease of the swirl at the rotor exit. As the deviation angle moves to the positive direction, the swirl increases which results in slightly lower efficiencies.

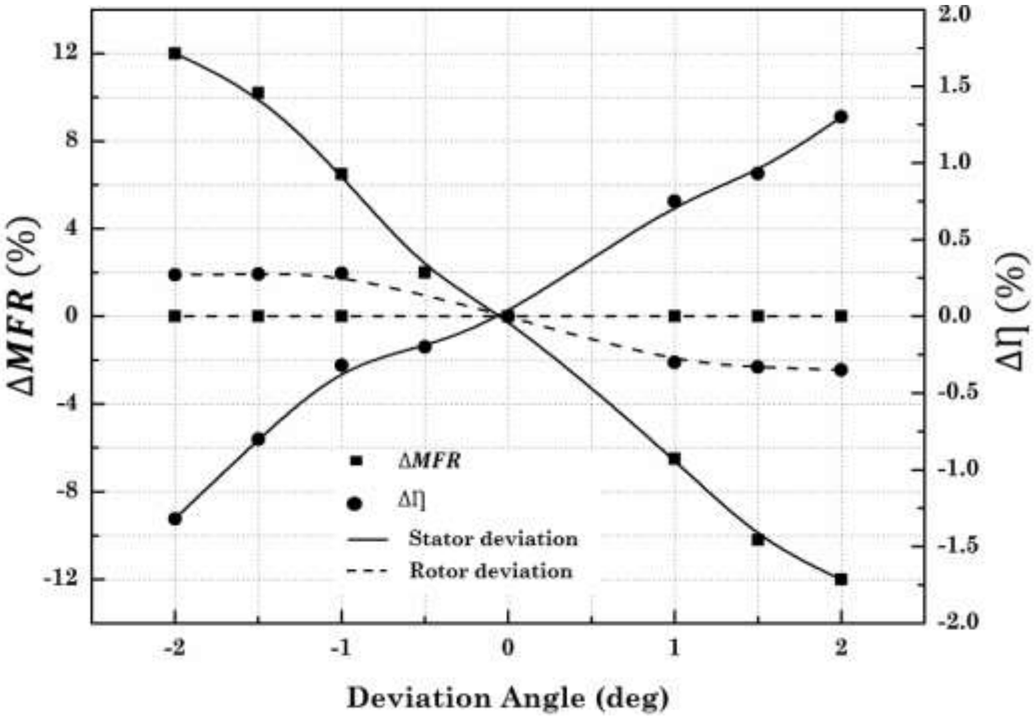

Fig. 16: Deviation of mass flow rate and turbine efficiency versus deviation angles

Last but not least, the rotor incidence angle is explored and the results are plotted in Fig. 17. According to the measurement of Woolley and Hatton [47], the flow becomes more uniform as the incidence angle moves from 0^o to negative values down to -40^o. Beyond -40^o, the flow separation appears again on the pressure side. Baines [48] concurred with Wooley and Hatton on the optimum incidence angle. He also stated that zero or positive incidence angle has the effect of reducing the cross-passage pressure gradient which results in flow separation on the suction surface. Moreover, Kline et al. [49] stated that positive incidence results in higher exit energy loss, leading to lower turbine efficiency. The results shown in Fig. 17 confirm the findings mentioned above. The best performance is achieved with the incidence angle in the range of -20^o to -40^o. At -50^o, the efficiency drops dramatically. At low pressure ratios (up to 1.75), the performance of the turbine is similar for different incidence angles. At higher values (PR > 1.75), the incidence angles -40^o, -20^o, and 0^o, respectively, show best performance.

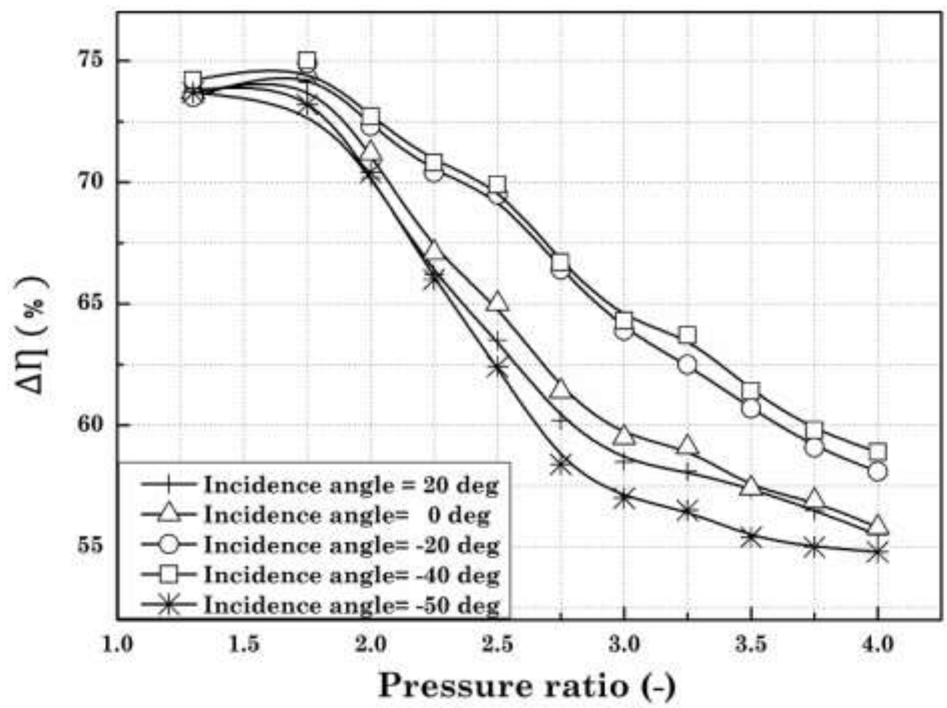

Fig. 17: Effects of incidence angle on turbine efficiency

Based on the results of the parametric study, optimum turbine performance is obtained with zero blockage factor. However, blocking is mandatory due to the blade thickness. Therefore, a value of BK = 0.1 is assigned for both stator and rotor as recommended by Moustapha et al. [56]. This value is considered realistic, although it affects the turbine flow capacity and efficiency, since it accounts for geometric blockage and boundary layers. Based on Fig. 16, the deviation angles for both stator and rotor are kept 0^o in order to maintain the same flow capacity through the turbine stage. An incidence angle of -40^o is chosen in the meanline model since it presents the optimum turbine performance as shown in Fig. 17.

4.3 Validation of the Method

Although the meanline model has been validated in Alshammari et al. [36], further validation is necessary due to some significant missing parameters in the testing case by Shao et al. [50]. One of the missing parameters is the rotor blade height which plays a vital role in the prediction of the flow capacity. The flow capacity or mass flow rate is the control parameter in the meanline model since it is firstly assumed at the beginning of the process and then validated at each station. Therefore, the mass flow rate is also a critical parameter at the prediction of the turbine efficiency. Another missing parameter is the stator opening (stator throat) which is very essential in estimating the flow velocity at the stator outlet, and the nature of the flow whether subsonic or supersonic. Unlike air turbines, radial turbines usually choke in ORC systems. In the previous testing case (Shao et al. [50]), mass flow rates were not plotted against pressure ratio. Therefore, there was no chance to assess the developed mass model. Although these data were missing, the maximum deviation between the predicted efficiency and measured efficiency using Shao et al. [50] was 7%.

The results of the meanline model are compared against the test results of the current study for three various speed lines i.e. 10,000 rpm, 15,000 rpm and 20,000 rpm. It is worth mentioning that the radial inflow turbine was designed mainly for this application considering the exhaust gas temperature of the engine at full load as the heat source for the thermal oil loop. In such consideration, the rotational speed of the design point is 40,000 rpm (Table 2). However, due to the limitation of the engine dynamometer, the engine is operating at partial load (81 kW instead of 206 kW) with a torque of 450 N.m and maximum speed tested (1700 rpm). Therefore, the turbine is tested at highly off-design conditions.

In Fig. 18, the model is validated against the experimental data for the three speed lines. Although efficiencies are mostly overestimated by the proposed meanline model, the general trend of the turbine efficiency is correctly reproduced.

The maximum deviation between the predicted and measured data is 3.50 % in the 15000 rpm speed line as depicted in Fig. 19. The turbine has been designed to operate at high pressure ratio (PR = 6). Fig. 18 shows that the meanline model is capable of estimating the turbine performance at pressure ratios near the design point value with relative error less 2.8%. At higher pressure ratios, the deviation is relatively high which suggests that the tested turbine may suffer some unusual effects at high pressure ratios.

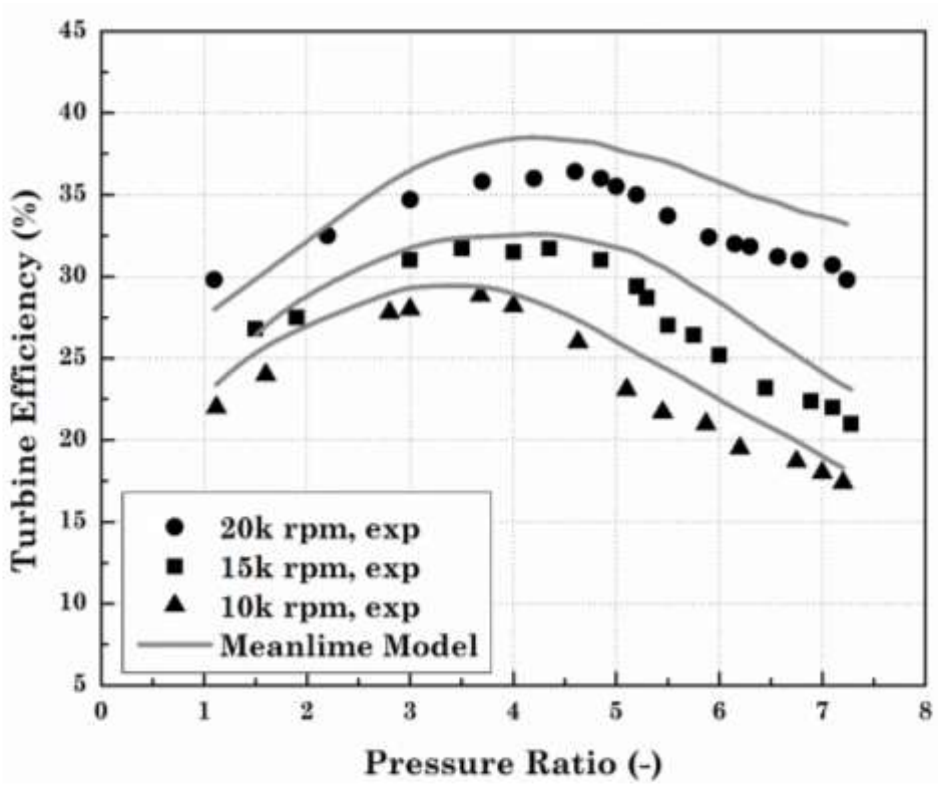

Fig. 18: Validation of the proposed meanline model

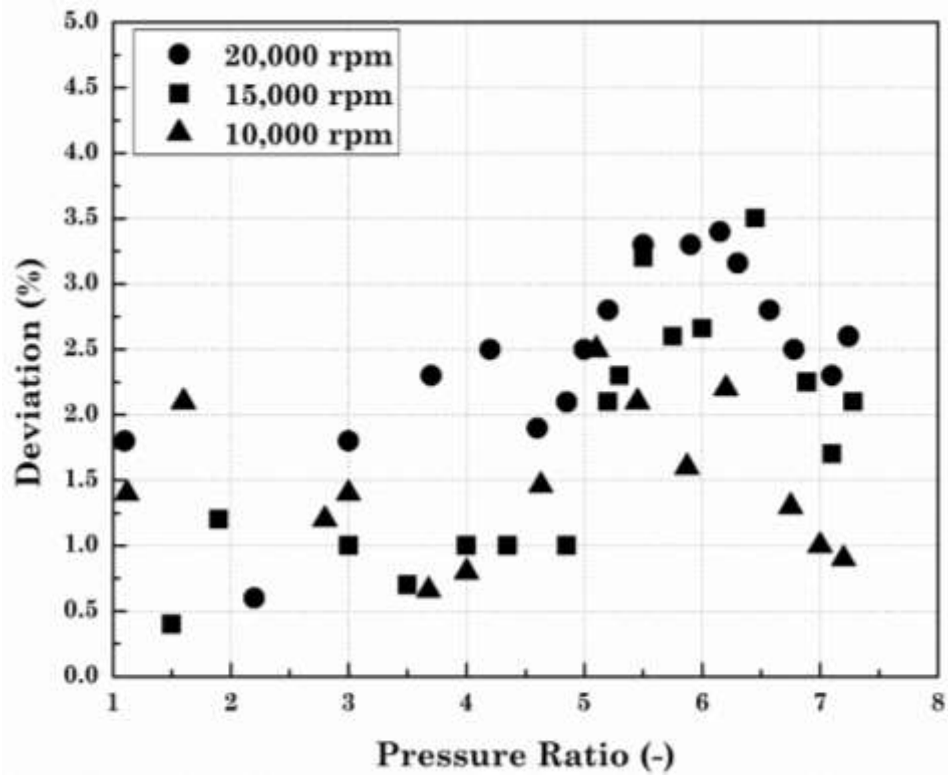

Fig. 19: Deviations between the tested and predicted results

In order to evaluate the proposed mass model, the comparison between tested and predicted mass flow parameter equation (1) versus pressure ratio is depicted in Fig. 20. The corrected mass flow rate is also known as mass flow parameter (MFP). As expected, the turbine chokes at $PR \geq 4.8$. The figure also assures the capability of the proposed mass model in predicting the occurrence of flow choking.

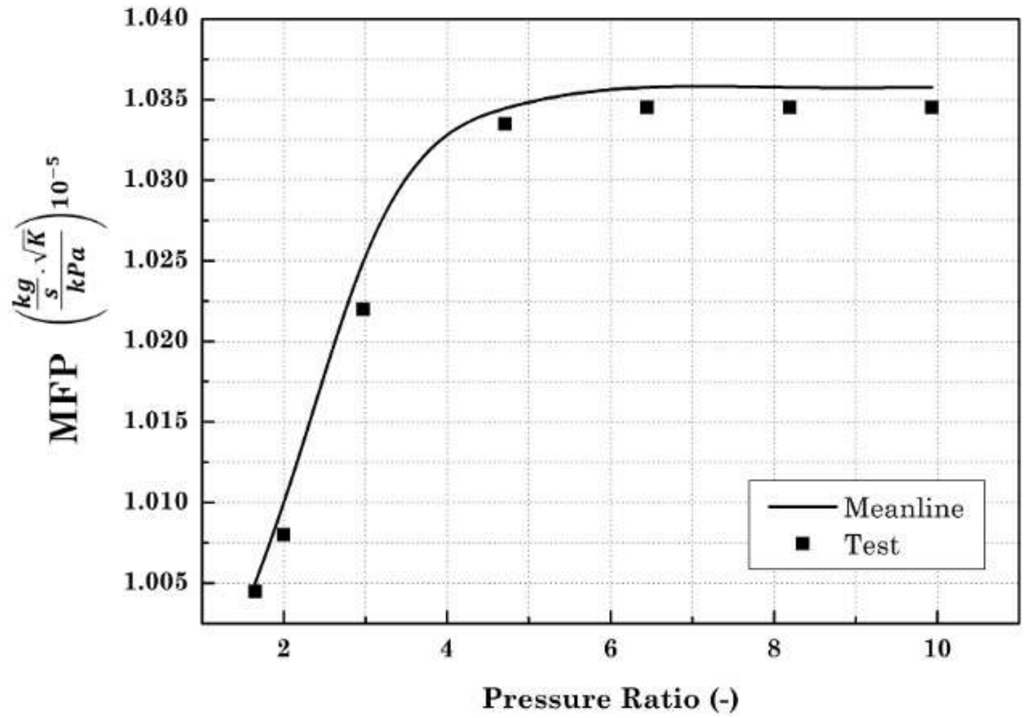

Fig. 20: Tested and predicted mass flow parameter versus pressure ratio

Since the experimental results confirmed the ability of the meanline model to produce turbine maps, the performance of the current turbine is estimated at extended range of operating points. Using the design point data available in Table 2, the turbine map is built as shown in Fig. 21. The figure clearly shows that the 40,000 rpm speed line (design point speed) presents more efficient turbine performance for the full range of operating pressure ratios.

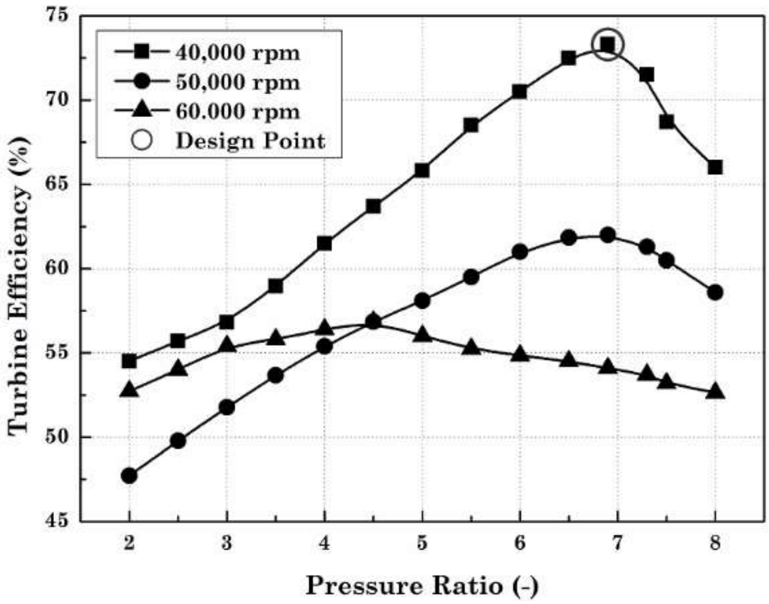

Fig. 21: Performance map of the custom-designed radial inflow turbine using the meanline model

5. Conclusion

In this paper, a compact ORC system, with a custom-designed radial turbine (and generator), coupled to heavy duty diesel engine was tested. The tests were run at engine partial load conditions considering the fact that off-design point is the frequent engine operating point. The ORC and the custom-designed radial inflow turbine presented a nearly constant efficiencies of 4% and 35%, respectively.

One of the main objectives of the paper was to explore the effects of cooling water temperature and fluid superheating temperature on the cycle performance. The results showed that increasing the cooling water temperature had a negative impact on the turbine performance. This was due to the decreased pressure ratio which affected both generated power and turbine efficiency. Similarly, increasing the superheating temperature, while fixing water flow capacity and temperature, deteriorated the turbine efficiency and generated power since the turbine pressure ratio presented a decreasing trend.

The results of the tests were applied in order to validate the previously developed performance prediction meanline model by authors [38]. The results of model were in good agreement with experimental results with a maximum deviation of 3.5% at 15000 rpm.

Acknowledgement

This work was supported by Innovate UK to this project [grant numbers. TS/M012220/1]. The authors would like to thank the assistance of Entropea Labs Limited in the preparation of the ORC test rig and subsequent experimental testing.

References

1. Johnson, T.V., *Diesel Emissions in Review.* SAE International Journal of Engines, 2011. **4**(1): p. 143-157.
2. Greenwald, J., *Oil Sands up Close*. 2012.
3. Department for, T., *Fuel Consumption*. 2013.
4. Hernandez, A., et al. *Towards the optimal operation of an Organic Rankine Cycle unit by means of model predictive control*. Brussels, Belgium.
5. Shu, G.-Q., et al. *Simulations of a Bottoming Organic Rankine Cycle (ORC) Driven by Waste Heat in a Diesel Engine (DE)*. SAE International.
6. Katsanos, C.O., D.T. Hountalas, and E.G. Pariotis, *Thermodynamic analysis of a Rankine cycle applied on a diesel truck engine using steam and organic medium.* Energy Conversion and Management, 2012. **60**(Supplement C): p. 68-76.
7. Shu, G., et al., *Analysis of regenerative dual-loop organic Rankine cycles (DORCs) used in engine waste heat recovery.* Energy Conversion and Management, 2013. **76**: p. 234-243.

8. Song, J. and C.-w. Gu, *Parametric analysis of a dual loop Organic Rankine Cycle (ORC) system for engine waste heat recovery.* Energy Conversion and Management, 2015. **105**: p. 995-1005.
9. Karvountzis-Kontakiotis, A., et al. *Variable Geometry Turbine Design for Off-Highway Vehicle Organic Rankine Cycle Waste Heat Recovery.*
10. Yang, M.-H. and R.-H. Yeh, *The effects of composition ratios and pressure drops of R245fa/R236fa mixtures on the performance of an organic Rankine cycle system for waste heat recovery.* Energy Conversion and Management, 2018. **175**: p. 313-326.
11. Rashwan, S.S., I. Dincer, and A. Mohany, *Analysis and assessment of cascaded closed loop type organic Rankine cycle.* Energy Conversion and Management, 2019. **184**: p. 416-426.
12. Di Battista, D., M. Mauriello, and R. Cipollone, *Waste heat recovery of an ORC-based power unit in a turbocharged diesel engine propelling a light duty vehicle.* Applied Energy, 2015. **152**: p. 109-120.
13. Li, P., et al., *Comparative analysis of an organic Rankine cycle with different turbine efficiency models based on multi-objective optimization.* Energy Conversion and Management, 2019. **185**: p. 130-142.
14. Endo, T., et al., *Study on Maximizing Exergy in Automotive Engines.* SAE TECHNICAL PAPER SERIES, 2007.
15. Zhang, H.G., E.H. Wang, and B.Y. Fan, *A performance analysis of a novel system of a dual loop bottoming organic Rankine cycle (ORC) with a light-duty diesel engine.* Applied Energy, 2013. **102**(Supplement C): p. 1504-1513.
16. Hossain, S.N. and S. Bari, *Waste heat recovery from the exhaust of a diesel generator using Rankine Cycle.* Energy Conversion and Management, 2013. **75**: p. 141-151.
17. Zhang, Y.-Q., et al., *Development and experimental study on organic Rankine cycle system with single-screw expander for waste heat recovery from exhaust of diesel engine.* Energy, 2014. **77**(Supplement C): p. 499-508.
18. Furukawa, T., et al., *A Study of the Rankine Cycle Generating System for Heavy Duty HV Trucks.* SAE Technical Paper, 2014.
19. Galindo, J., et al., *Experimental and thermodynamic analysis of a bottoming Organic Rankine Cycle (ORC) of gasoline engine using swash-plate expander.* Energy Conversion and Management, 2015. **103**(Supplement C): p. 519-532.
20. Yu, G., et al., *Experimental investigations on a cascaded steam-/organic-Rankine-cycle (RC/ORC) system for waste heat recovery (WHR) from diesel engine.* Energy Conversion and Management, 2016. **129**: p. 43-51.
21. Guillaume, L., et al., *Performance of a Radial-Inflow Turbine Integrated in an ORC System and Designed for a WHR on Truck Application: An Experimental Comparison between R245fa and R1233zd.* Applied Energy, 2017. **186**: p. 408-422.
22. Glensvig, M., et al. *Testing of a Long Haul Demonstrator Vehicle with a Waste Heat Recovery System on Public Road*. SAE International.
23. Sellers, C., *Field operation of a 125kW ORC with ship engine jacket water.* Energy Procedia, 2017. **129**(Supplement C): p. 495-502.
24. Shi, L., et al., *Experimental comparison between four CO2-based transcritical Rankine cycle (CTRC) systems for engine waste heat recovery.* Energy Conversion and Management, 2017. **150**: p. 159-171.

25. Alshammari, F., et al., *Experimental study of a small scale organic Rankine cycle waste heat recovery system for a heavy duty diesel engine with focus on the radial inflow turbine expander performance.* Applied Energy, 2018. **215**: p. 543-555.
26. Linnemann, M., et al., *Design and test of a multi-coil helical evaporator for a high temperature organic Rankine cycle plant driven by biogas waste heat.* Energy Conversion and Management, 2019. **195**: p. 1402-1414.
27. Alshammari, F., et al., *Expander Technologies for Automotive Engine Organic Rankine Cycle Applications.* Energies, 2018. **11**(7).
28. White, M., *The design and analysis of radial inflow turbines implemented within low temperature organic Rankine cycles*. 2015.
29. Wong, C.S., *Design Process of Low Temperature Organic Rankine Cycle (LT-ORC)*. 2015.
30. Jansen, W. and E.B. Qvale, *A Rapid Method for Predicting the Off-Design Performance of Radial-Inflow Turbines.* ASME -PUBLICATIONS-, 1967(80067): p. V001T01A002-V001T01A002.
31. Dadone, A. and M. Pandolfi, *A method for evaluating the off-design performance of a radial inflow turbine and comparison with experiments.* International Journal of Mechanical Sciences, 1969. **11**(3): p. 241-252.
32. Ghosh, S.K., *Experimental and Computational Studies on Cryogenic Turboexpander*. 2008.
33. Baines, N.C., *A Meanline Prediction Method for Radial Turbine Efficiency," in 6th International Conference on Turbocharging and Air Management Systems.* Concepts ETI, Inc, 1998.
34. Whitfield, A. and N.C. Baines, *Design of Radial Turbomachines*. 1990: Longman Scientific and Technical, Harlow, England.
35. Rodgers, C. and R. Geiser, *Performance of a High-Efficiency Radial/Axial Turbine.* Journal of Turbomachinery, 1987. **109**(2): p. 151-154.
36. Alshammari, F., et al., *Off-design performance prediction of radial turbines operating with ideal and real working fluids.* Energy Conversion and Management, 2018. **171**: p. 1430-1439.
37. Borsukiewiczgozdur, a. and W. Nowak, *Comparative analysis of natural and synthetic refrigerants in application to low temperature Clausius–Rankine cycle.* Energy, 2007. **32**(4): p. 344-352.
38. Dong, B., et al., *Parametric analysis of organic Rankine cycle based on a radial turbine for low-grade waste heat recovery.* Applied Thermal Engineering, 2017. **126**(Supplement C): p. 470-479.
39. Liu, B.T., K.H. Chien, and C.C. Wang, *Effect of working fluids on organic Rankine cycle for waste heat recovery.* Energy, 2004. **29**(8): p. 1207-1217.
40. Franchetti, B., et al. *Thermodynamic and technical criteria for the optimal selection of the working fluid in a mini-ORC.*
41. Karvountzis-Kontakiotis, A., et al., *Effect of an ORC Waste Heat Recovery System on Diesel Engine Fuel Economy for Off-Highway Vehicles*. 2017.
42. Life, M.S.A.t., *Organic Fluids*.
43. Stobart, R. and R. Weerasinghe, *Heat Recovery and Bottoming Cycles for SI and CI engines - A Perspective.* SAE Techinical Paper 2006-01-0662, 2006. **2006**(724).
44. Tian, H., et al., *Fluids and parameters optimization for the organic Rankine cycles (ORCs) used in exhaust heat recovery of Internal Combustion Engine (ICE).* Energy, 2012. **47**(1): p. 125-136.

45. Benson, R.S., *An Analysis of the Losses in a Radial Gas Turbine.* Proceedings of the Institution of Mechanical Engineers, Conference Proceedings, 1965. **180**(10): p. 41-53.
46. Pullen, K.R., N.C. Baines, and S.H. Hill, *The Design and Evaluation of a High Pressure Ratio Radial Turbine.* ASME Publication, 1992(78934): p. V001T01A050-V001T01A050.
47. Woolley, H. and P. Hatton. *viscous flow in radial turbomachine blade passages*.
48. Baines, N.C. *Flow Development in Radial Turbine Rotors*.
49. Kline, J.F., T.P. Moffitt, and R.G. Stabe, *Incidence Loss for Fan Turbine Rotor Blade in Two-Dimensional Cascade*. 1983, NASA: Cleveland, OH, United States.
50. Shao, L., et al., *Experimental study of an organic Rankine cycle system with radial inflow turbine and R123.* Applied Thermal Engineering, 2017. **124**(Supplement C): p. 940-947.